Chemical Engineering Journal 166 (2011) 15–21

Contents lists available at ScienceDirect

Chemical Engineering Journal

journal homepage: www.elsevier.com/locate/cej

Preparation and characteristics of a nano-PbO_2 anode for organic wastewater treatment

Chao Tan, Bo Xiang*, Yijiu Li, Jianwei Fang, Min Huang

Department of Chemistry, Tongji University, 1239 Siping Road, Shanghai 200092, People's Republic of China

ARTICLE INFO

Article history:
Received 19 June 2010
Received in revised form 10 August 2010
Accepted 10 August 2010

Keywords:
Nano-PbO_2 anode
Electrochemical oxidation
Chloride ion
Organic wastewater treatment

ABSTRACT

A nano-PbO_2 anode (PbO_2/NT) was prepared by a pulse electrodeposition (PED) method. Self-organized TiO_2 nanotube (NT) arrays were produced by electrochemical anodization and used as a substrate to load PbO_2 by PED method. The morphological and structural properties were studied by the field-emission scanning electron microscopy and X-ray diffraction revealing successful deposition of lead dioxide nanoparticles on the NT walls. The electrochemical activity of PbO_2 loaded on TiO_2 nanotube arrays electrode (PbO_2/NT) was found to be influenced by the length of electrochemical plating time. Chronoamperometric experiments showed that PbO_2/NT anodes possessed stronger oxidation ability than that of traditional PbO_2 anodes (PbO_2/Ti). PbO_2/NT, due to its unique microstructure, could oxidize chlorine effectively under basic conditions. The effect of current density on total organic carbon (TOC) removal by PbO_2/NT varied with different organic reactants used. The TOC removal rate of isopropanol was controlled by mass transfer, while the removal rate of 4-chlorophenol (4-CP) was mainly influenced by passivation. The synergistic effects of pH, flow rate, and supporting electrolyte on the TOC removal percentage using PbO_2/NT or PbO_2/Ti were investigated as well.

1. Introduction

The increasing emission of refractory organic pollutants has challenged the conventional biological treatment because they, unlike other compounds in wastewater, possess high resistance to microbial degradation or utilization. To meet increasingly rigorous discharge limits, these effluents must be treated by technologically advanced treatment systems. In recent years, a large number of studies have been focusing on developing new technologies for the treatment of industrial wastewater contaminated with organic compounds [1–5]. Electrochemical oxidation has been found to be a promising technology for treating wastewater containing refractory organic pollutants and has drawn significant attention in water treatment research [6–8], because of its environmental compatibility, small space requirement, and powerful oxidation ability [9–11].

However, electrochemical oxidation faces economical inefficiencies that derive from both operating cost and anodes preparation cost. The anode material is crucial in reducing the cost of electrochemical oxidation method [12,13]. In recent decades, a lot of electrode materials have been examined to improve the effectiveness of oxidation and current efficiency, such as graphite [14], platinum [15], IrO_2 [16], RuO_2 [17], SnO_2 [18], PbO_2 [19], and boron-doped diamond (BDD) electrodes [13]. When using platinum anodes, a large amount of current supplied will be wasted in production of oxygen, leading to a low current efficiency. The IrO_2 and RuO_2 electrodes had low reactivity for organic oxidation. So far, many studies have pointed out that BDD anodes allow complete mineralization without sharply decreasing current efficiency [20,21] but their preparation is complicated and costly especially for that with a large area. The graphic anodes are inexpensive but they have low current efficiencies due to their low overpotential of oxygen evolution. SnO_2 anodes have an obvious shortcoming-relatively short service life though their overpotential of oxygen evolution is higher than graphic anodes. So there is a need to develop anodes of both high oxidative activities and low costs. PbO_2 anodes are potential candidates to meet this criterion. They have high overpotentials for oxygen evolution, a strong ability to produce hydroxyl radicals, and very good conductivity. However, PbO_2 anodes do not have satisfactory electrocatalytic ability compared with BDD anodes. To solve this problem, recent research has focused on modification of PbO_2 anodes by element doping, such as Bi [22,23], Co [24], Ce [25,26], Fe [27], PTFE [28], and F [29,30].

This paper is focused on a novel way to increase the electrocatalytic activity of PbO_2 anodes. The traditional substrate of PbO_2 anodes is usually Ti. An attempt on substrate substitution was carried out in this research. The vertically aligned TiO_2 nanotube arrays (TiO_2 NT arrays), with a larger surface area than Ti substrate, can serve as a novel underlay for PbO_2. TiO_2 NT arrays can be fabri-

* Corresponding author.
E-mail address: tongxunzuozhe@gmail.com (B. Xiang).

1385-8947/$ – see front matter © 2010 Elsevier B.V. All rights reserved.
doi:10.1016/j.cej.2010.08.018

cated by anodic oxidation of Ti substrate in fluoride containing electrolytes and remain attached on the substrate [31]. The nanoarchitecture of NT arrays features a high surface-to-volume ratio, which is due to the additional area enclosed inside the hollow structure. To the best of our knowledge, few studies on the direct loading of PbO_2 onto TiO_2 NT arrays have been reported. Once the metal oxide active layer can enter the internal area of TiO_2 NT arrays, it can reach nanoscale and be highly dispersed due to the restriction of nano-tubular structure [32]. It is not easy to deposit PbO_2 into TiO_2 NT arrays by constant current electrodeposition due to the high surface tension of the NT. The pulse electrodeposition (PED) technique was employed to synthesize highly-ordered TiO_2 NT arrays loaded with PbO_2 electrode (PbO_2/NT).

Since most industrial effluents containing high chloride concentrations, the other aim of this research is to compare the electrocatalytic performance of PbO_2/NT with that of PbO_2/Ti with respect to their abilities to degrade organic contaminants in the presence of sodium chloride. Two kinds of organic molecules were chosen as the model reactants. One is 4-chlorophenol (4-CP) which is a priority pollutant and ubiquitous in the environment [33]. It is used widely in agricultural and non-agricultural purposes, yielding waste product and contaminating soil in application sites [34]. The other model reactant selected in this study is isopropanol. This compound was selected because it can be easily degraded due to its short-chain simple structure, and thus would not cause appreciable passivation of the electrode during electrochemical incineration. Additionally, the oxidation of a simple molecule does not typically generate large amounts of stable intermediates that otherwise interfere with the analysis of experimental results. The influence of pH and flow rate on TOC (total organic carbon) removal in the presence of NaCl was investigated in this study.

2. Experimental details

Acetone, diethylene glycol (DEG), hydrofluoric acid 40%, $(NH_4)_2SO_4$, Na_2SO_4, NaCl, isopropanol and 4-chlorophenol were obtained from Sinopharm Chemical Reagent Co., Ltd. All the chemicals reagents were of analytical grade and used without further purification.

2.1. Electrode preparation

2.1.1. PbO_2/NT electrode preparation

The titanium sheets (1.0 mm thickness, 99.5% purity) were mechanically polished using abrasive papers of successively finer roughness (100, 400 and 800 grit) and then rinsed in two 15 min steps in ultrasonicated acetone and deionized distilled water (DDW) before drying in flowing N_2 stream. Anodization experiments were conducted using a two-electrode electrochemical cell, in which the titanium sheet was used as the anode and a platinum foil of similar size was used as the cathode. The gap between anode and cathode was fixed at 2 cm. After 10 h of anodization at 60 V in the 1.4 wt% HF/diethylene glycol (DEG) solution, the as-prepared sample was washed with DDW. It was placed into a methanol bath for several hours to avoid surface cracks and peeling [35]. After that, the initially amorphous TiO_2 NT arrays were crystallized by annealing at 550 °C in N_2 atmosphere for 1 h.

The TiO_2 NT arrays are not suitable for electrodeposition due to their semiconductive nature. In order to increase their conductivity, the TiO_2 NT arrays were electrochemically reduced for 8 s in 1 M $(NH_4)_2SO_4$ at a potential of −1.5 V versus Ag/AgCl electrode [36]. Then PbO_2 was deposited onto the TiO_2 NT substrate by PED technique [37] using the Autolab PGSTAT-30 electrochemical analysis system with General Purpose Electrochemistry System version 4.9 software package (Eco Chemie B.V., The Netherlands). The TiO_2 NT arrays were used as a working electrode, Ag/AgCl (1 M KCl) as a reference electrode, and a Pb mesh as a counter electrode. The PbO_2 electrodeposition bath was a mixture of 0.1 M HNO_3, 0.5 M $Pb(NO_3)_2$, 0.02 M NaF, 60 °C. The length of electrochemical plating time varied from 10 to 100 min.

2.1.2. PbO_2/Ti electrode preparation

The PbO_2/Ti electrode was fabricated similarly to the PbO_2/NT electrode. However, the anodization process in HF solution was excluded. The length of electrochemical plating time for the PbO_2/Ti is 70 min.

2.2. Electrochemical measurement

All the electrochemical experiments were performed at 20 ± 2 °C. The working anodes were tested for their cyclic voltammetry (CV) and chronoamperometry by Autolab PGSTAT-30 electrochemical analysis system, using the General Purpose Electrochemistry System version 4.9 software package. The reference electrode was an Ag/AgCl (1 M KCl). In order to investigate the effect of the length of electrochemical plating time, the method of CV have been applied in the solution containing 1 mM 4-CP and 0.1 M NaCl. The PbO_2/NT anodes with different length of electrochemical plating time were used as working electrodes. During a series of chronoamperometric tests, the solutions contain Na_2SO_4 and x mM NaCl (where x = 0, 10, 30, 60, 90, 300), pH = 2.5 ± 0.1 or 11.5 ± 0.1.

2.3. Electrochemical degradation

The effect of current density was evaluated by the degradation experiments of 4-CP and of isopropanol respectively. The degradation experiment of 4-CP was carried out in an undivided electrochemical cell at 20 ± 2 °C. The initial concentrations of 4-CP was selected as 1.00 g l^{-1} with a volume of 200 ml. The surpporting electrolyte was 5.84 g l^{-1} NaCl. The condition of degradation experiment of isopropanol was similar to 4-CP. The PbO_2/NT with wet surface area of 16 cm^2 was used as the anode and the titanium sheet with the same wet surface area was used as the cathode. Prior to the TOC analysis (TOC-Vcpn, Shimadzu, Japan), samples from the treated solution were filtered with 0.45 μm polytetrafluoroethylene (PTFE) membrane to remove any solid generated during the degradation. Filtering the sample will allow the fluctuation of the TOC measurement to be kept at less than ±1 mg l^{-1}.

The effect of pH and flow rate was examined in a dynamic system that consisted of a 50 ml cell, a 200 ml reservoir and a peristaltic pump. The cell, reservoir and pump were connected serially to form a hydraulic circuit. The degradation solution was pumped from the reservoir through the cell and back to the reservoir in a closed loop. The PbO_2/NT and the PbO_2/Ti were employed as the working electrode with both wet surface area of 16 cm^2. The cathode was titanium sheet with the same area of working electrode. Comparative degradation experiments of isopropanol (250 ml 1000 mg l^{-1}) with 0.1 M NaCl at different pH (2.5 and 11.5) and different flow velocity (60 and 600 ml min^{-1}) were carried out. The applied current density was set at 15 mA cm^{-2}. Electrolysis test proceeded until the total passed charge reached 4000 coulombs.

3. Results

3.1. Morphology of PbO_2/NT anode

Fig. 1 shows top-down views of representative field-emission SEM images. As illustrated in Fig. 1a, the in situ grown TiO_2 NT arrays consists of well-aligned, uniform, cylindrical tubes that extend down to the titanium substrate. The average inner tube

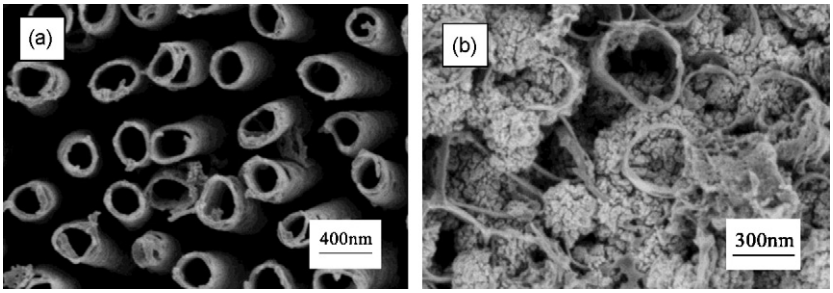

Fig. 1. Field-emission SEM (FESEM) top-view image of (a) TiO_2 nanotube arrays and (b) PbO_2/NT anode.

diameter is about 220 nm. The highly-ordered TiO_2 NT arrays possess high specific volume and large surface area. Fig. 1b shows how TiO_2 NT arrays are fully absorbed with PbO_2 nanoparticles. Comparison of two FESEM images before and after electrodeposition in Fig. 1 clearly certify the effectiveness of PED method. It is effective for the formation of PbO_2 nanoparticles and the electrodeposition into the TiO_2 NT. To identify the chemical and structural nature of the deposits, XRD measurements were performed. Fig. 2 gives the X-ray diffraction spectra for the PbO_2/NT anode. It consists of β-phase PbO_2 crystalline phase and titanium. According to the literature [38], the doping of fluorine ions in PbO_2 will not effect β-phase PbO_2 crystallgraphic form significantly in comparison with undoped PbO_2. The fluorine-doping PbO_2 anodes have higher onset overpotential for oxygen evolution and higher stability during that process. This is due to fluorine ions modification might take up the channels for diffusion of free oxygen atoms. The diffraction peak width is inversely proportional to crystallite size [39]. The average crystallite size was calculated from the full width at the half maximum (FWHM) of diffraction lines using the Scherrer equation. It was around 15 nm, which is smaller than the reported crystallite size of the lead dioxide anode [40] prepared by constant current electrodeposition. The smaller the catalytic particle is, the larger the surface area it posses and as a result of that, higher catalytic activity is readily accessible.

3.2. The effect of the length of electrochemical plating time

In Fig. 3, it is clear that the 70 min electrodeposited PbO_2/NT has the highest anodic peak, corresponding to the direct oxidation of 4-CP. The anodic peak of the electrode that was only exposed to 10 min of electrodeposition time appears very small. It is well known that lead dioxide electrode has a very strong ability in hydroxyl radical production, which is even stronger than the BDD anode [41]. The most of the hydroxyl radicals that produced by lead dioxide electrode were absorbed hydroxyl radicals. They would react with organic compounds near the surface of the lead dioxide electrode, causing the diminishing of adsorbed hydroxyl radicals on the surface of PbO_2. The removal of hydroxyl radicals from the active sites promotes the discharge of water, resulting in the appearance of anodic peak [42]. The peak currents of the four PbO_2/NT anodes demonstrates that the different electrooxidation activity for 4-CP on these four anodes proceeds in the following order from high to low: PbO_2/NT 70 min, PbO_2/NT 100 min, PbO_2/NT 40 min and PbO_2/NT 10 min. An increase of the electrodeposition time up to 70 min can give rise to an increment of peak current. However, when deposition time was 100 min, an opposite trend of peak current emerges. This phenomenon indicates that there is an optimum load capacity of PbO_2 for PbO_2/NT. The number of active sites for hydroxyl radical production increased as the length of plating time at first. When the length of plating time was shorter than 70 min, the longer the plating time the stronger the oxidation ability of PbO_2/NT. However, the activity of PbO_2/NT declined when the length of deposition time was 100 min. We observed that the amount of PbO_2 loading on substrate is increasing with the growing of deposition time (the specific data not shown), and therefore we suggest that an optimum length of electrodeposition time exists. Any time that is longer than the optimum length may cause PbO_2 to be overloaded on TiO_2 NT arrays. The excess PbO_2 blocked or covered the NT arrays, resulting in a decrease of specific surface area of PbO_2/NT anodes as well as the active sites. The oxidation peak current on the PbO_2/NT 70 min reached 6.1 mA cm^{-2}, which was much larger than 2.6 mA cm^{-2} on the PbO_2/Ti 70 min. This suggests that PbO_2/NT is more active than PbO_2/Ti because PbO_2 is dispersed more effectively on the TiO_2

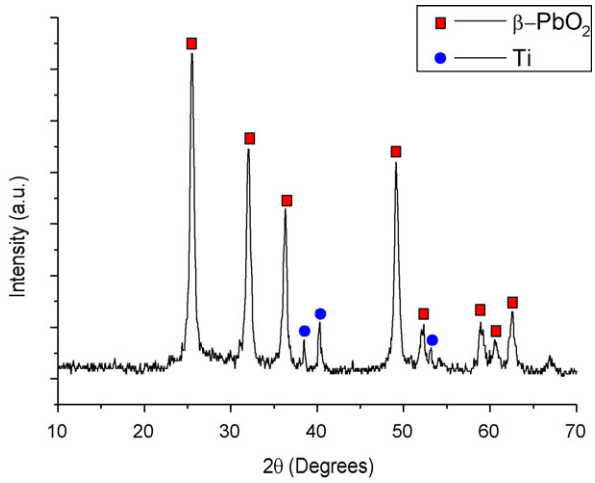

Fig. 2. X-ray diffraction pattern of PbO_2/NT anode.

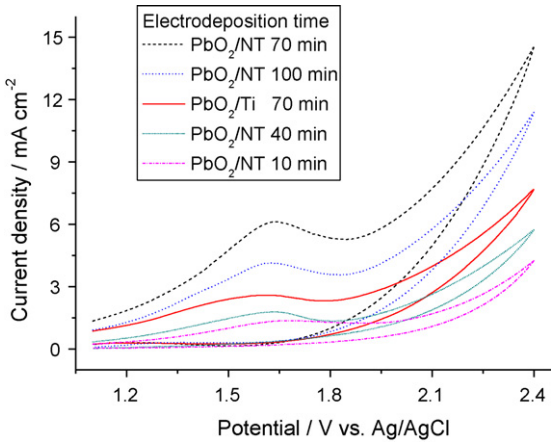

Fig. 3. Cyclic voltammograms of PbO_2/NT and PbO_2/Ti obtained at different electro deposition time in 1 mM 4-CP + 0.1 M NaCl. Scan rate: 0.1 V/s. $T = 20 \pm 2$ °C.

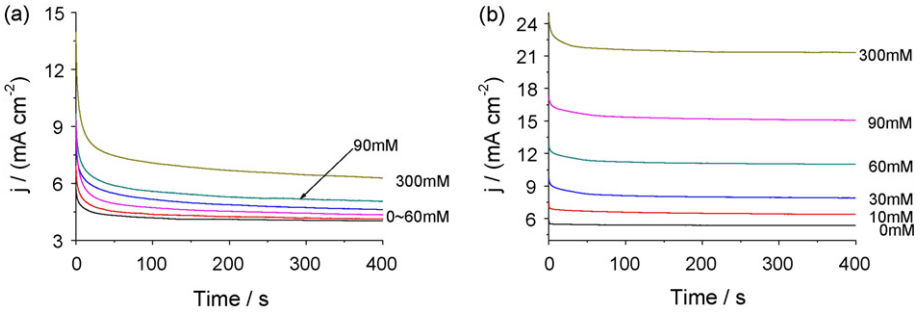

Fig. 4. Chronoamperometric curves recorded at various NaCl concentration with pH = 2.5. (a) PbO_2/Ti. (b) PbO_2/NT.

NT arrays substrate than on the Ti substrate. As for PbO_2/Ti, PbO_2 nanoparticles are distributed merely on the top surface of Ti sheet. For PbO_2/NT, however, not only the top surface but also the inner and outer wall surface of NT is the site for PbO_2 nanoparticles loading. Therefore, more activated centers of PbO_2 nanoparticles can be exposed for reaction.

3.3. Chronoamperometric experiments

In the acidic system with initial pH of 2.5, the current density increased with the increasing concentration of sodium chloride ([NaCl]) both on the PbO_2/Ti and the PbO_2/NT (Fig. 4). This may be due to chloride oxidation being favorable under acidic condition. A similar result was observed on the PbO_2/NT at pH of 11.5 regardless of the fact that chloride oxidation was not the main contributor to current increase in basic conditions (Fig. 5b). One could attribute this consequence to the special porous microstructure of PbO_2/NT. Though the alkaline pH of the bulk electrolyte would restrain chloride oxidation, the pH in NT could be low owing to oxygen evolution reaction (OER) and mass transfer limitations blocking the solution in NT from the bulk electrolyte outside NT. Thus, the pH in NT is not sensitive to the pH of the bulk of the solution. Furthermore, as shown in Fig. 5b, the current density dropped drastically during the initial tens of seconds of the chronoamperometic measurement, especially at low halide concentrations of 0, 10 and 30 mM. This may be due to the pH decline resulting from oxygen evolution.

The results gained from pH 11.5 at the PbO_2/Ti (Fig. 5a) exhibit a distinctive phenomenon, which is similar to the result of [43]. From 10 mM NaCl to 60 mM NaCl, the chronoamperometry responses shift towards lower levels with the increase of chloride concentration; above 90 mM a reversal of the trend appears. When the halide concentration is 90 mM, the current density was found to be higher than those of 10, 30 and 60 mM. This experiment found that the current response of 300 mM was the highest. To understand the physical meaning behind this phenomenon, oxygen and chlorine evolution reactions and their equilibrium potentials in the chloride containing system may be considered as below:

$$2Cl^- \rightarrow Cl_2 + 2e, \quad \varphi^{\Theta} = 1.358\,V$$

$$\text{Basic}: 4OH^- \rightarrow 2H_2O + O_2 + 4e, \quad \varphi^{\Theta} = 0.401\,V$$

$$\text{Acidic}: 2H_2O \rightarrow O_2 + 4H^+ + 4e, \quad \varphi^{\Theta} = 1.229\,V$$

The equilibrium potential of OER will shift towards negative if the pH of the system increases [44], which would result in OER more likely taking place. Thus the current density in the basic pH (Fig. 5a) is larger than in the acidic pH (Fig. 4a). The current density in the 10 mM NaCl case was lower than in the case of 0 mM NaCl in Fig. 5a. This is due to the anodic shift of the OER caused by adsorption of Cl^- at the anodic surface [43]. The extent of current density drop was gradually slowed down when [NaCl] increased to 30 and 60 mM in sequence. This might be due to the importance of [NaCl] to chlorine evolution under high Cl^- concentration. When [NaCl] was 90 mM, its promoting effect on chlorine evolution would be greater than its suppressing effect on OER. Therefore, the apparent current density increases.

It was found that current density on the PbO_2/NT was larger than on the PbO_2/Ti regardless of solution pH. This result indicates that after changing surface morphology of substrate for electrodeposition, the resulting PbO_2/NT had more active sites compared with PbO_2/Ti. Moreover, the highly-ordered TiO_2 NT arrays with three-dimensional network permits facile charge transfer along the length of the NT from the conductive substrate to the solution. Therefore it is possible to reduce the current losses resulting from charge-hopping across the nanoparticle grain boundaries [45]. The vertical tube microstructure allows efficient charge transfer [46].

3.4. Bulk electrolyses

3.4.1. The effect of current density

Fig. 6a plots several 4-CP degradation curves at constant current density in the range between 3 and 80 mA cm^{-2}. It is not

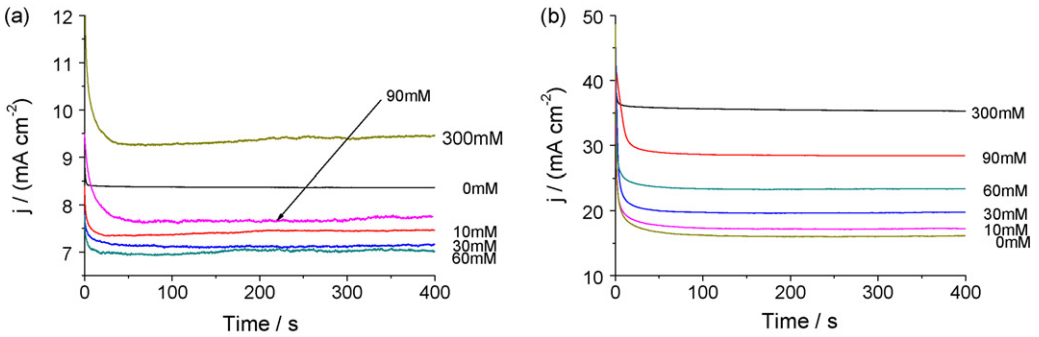

Fig. 5. Chronoamperometric curves recorded at various NaCl concentration with pH = 11.5. (a) PbO_2/Ti. (b) PbO_2/NT.

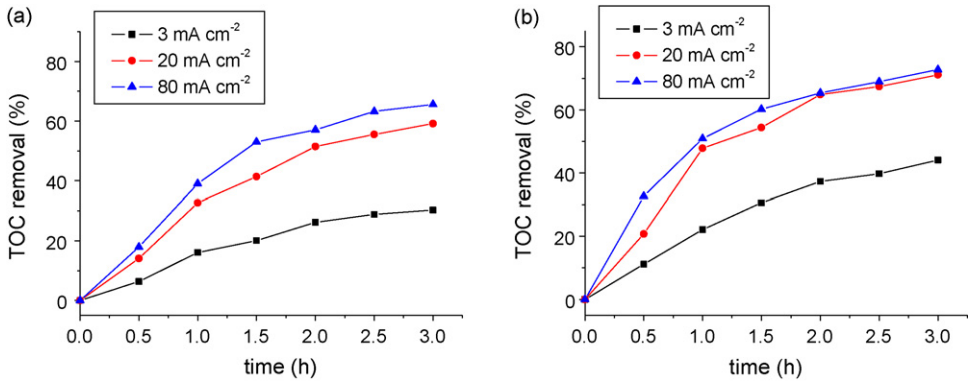

Fig. 6. Percentage of TOC removal as a function of degradation time for (a) 200 ml 1000 mg L^{-1} 4-chlorophenol in 0.1 M NaCl. (b) 200 ml 1000 mg L^{-1} isopropanol in 0.1 M NaCl.

difficult to find that under the similar condition the TOC removal rate is much higher than platinum anode according to Ref. [47]. Moreover, compared with the optimum result of nickel-antimony doped tin oxide electrode in Ref. [48], the TOC removal result of PbO_2/NT anode under 3 mA cm^{-2} is better. From Fig. 6 we can see that as applied current density increases, removal rate of 4-CP increases. This is because more charge is passed into the system, which leads to the generation of more hydroxyl radicals and active chlorine. However, in Fig. 6b, the removal rate of isopropanol only slightly increased when the current density increased from 20 to 80 mA cm^{-2}. The difference in removal rate with increasing current density shown by the two different organic compounds can be explained in aspects as side reaction and mass transfer limitation. As is known, the electrogenerated hydroxyl radicals can evolve to oxygen or peroxide which is a weaker oxidant towards organic species [49]. Though a larger amount of hydroxyl radicals were produced when increasing the current density from 20 to 80 mA cm^{-2}, a greater proportion of hydroxyl radicals was consumed by non-oxidizing waste reactions due to mass transfer limitation. As for the degradation of 4-CP, Azzam et al. [50] found that the rate of 4-CP degradation process was not in mass transfer control, thus electrode passivation should be considered. During the electrolysis at a potential lower than that required for OER to occur, the surface of anodes might be poisoned as a result of an electrogenerated polymer layer. The degree of passivation was greater under low current density than under high current density because the OER was less severe. Oxygen generated by the OER could mechanically remove the polymeric film adsorbed on the anode surface, and hence it is beneficial to prevent complete deactivation of the anode [51,52]. When a low current density was applied, the electrochemical reaction was not as influenced by the mass transfer limitation as the passivation on anode's surface. From this aspect, it is not hard to understand why the TOC removal rate of 20 mA cm^{-2} was not as high as 80 mA cm^{-2}.

Anode passivation could be confirmed by CV measurements (Fig. 7). Fig. 7a exemplifies five cycles of CV curve in 1 mM 4-CP solution with 0.1 M NaCl (pH 6.4). The oxidation peak appeared near 1.6 V in the first cycle, corresponding to the direct oxidation of 4-CP. Anodic peak current diminished in successive cycles, suggesting the rapid formation of an intermediate that can adhere to the electrode surface causing anode contamination. This phenomenon was in line with earlier worker [48], who attributed the early deactivation to the adsorption of the anodic products on the electrode active sites.

A new set of CV measurement was carried out in 1 mM isopropanol solution with 0.1 M NaCl (Fig. 7b). As expected in introduction, a slight passivation was observed in Fig. 7b. The size of the anodic peak near 1.4 V remained until the last cycle of scan. Meanwhile, the change of the area of the voltammograms was not evident.

3.4.2. *The effect of pH and flow rate*

To investigate the effect of pH and flow rate on the TOC removal percentage, a series of degradation experiments was carried out under different operating parameters in a dynamic system containing 250 ml 1.00 g l^{-1} isopropanol and 5.84 g l^{-1} NaCl (Table 1).

The effects of pH and flow velocity on isopropanol degradation were dependent on the anode species (PbO_2/NT and PbO_2/Ti) and the supporting electrolytes (Na_2SO_4 and NaCl). The electrolysis experiment with NaCl as the supporting electrolyte has a higher TOC removal percentage than the one with Na_2SO_4. The higher TOC removal may be due to the generation of active chlorine species: hypochlorous acid (HOCl), hyperchlorite (OCl^-), chlorine radical ($Cl^{\bullet}$), and dichloride radical anion ($Cl_2^{\bullet -}$) [53]. The role of pH can be

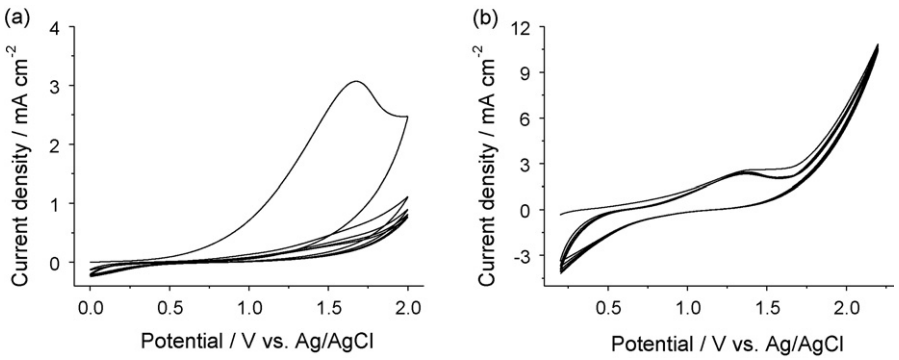

Fig. 7. Cyclic voltammograms obtained at PbO_2/NT for five cycles, starting with an anodic sweep. Scan rate: 0.2 V/s. $T = 20 \pm 2$ °C. (a) 1 mM 4-CP + 0.1 M NaCl. (b) 1 mM isopropanol + 0.1 M NaCl.

Table 1
The effect of pH and flow rate on TOC removal percentage using PbO_2/NT or PbO_2/Ti.

Supporting electrolyte	pH	Flow rate (ml/min)	TOC removal (%)	
			PbO_2/NT	PbO_2/Ti
0.1 M Na_2SO_4	2.5	60	18.3	16.6
0.1 M Na_2SO_4	2.5	600	29.7	28.0
0.1 M Na_2SO_4	11.5	60	13.5	10.6
0.1 M Na_2SO_4	11.5	600	22.3	17.9
0.1 M NaCl	2.5	60	56.2	50.6
0.1 M NaCl	2.5	600	60.4	57.3
0.1 M NaCl	11.5	60	40.7	16.8
0.1 M NaCl	11.5	600	24.1	23.4

explained by the following reasons. First, a decrease in pH increases the production of hydroxyl radicals, which increases the rate of oxidation [54]. Also, the reaction between intermediates and hydroxyl radical produced on the anode surface was faster under acidic pH. A similar result was obtained by Flox et al. [55] on a boron-doped diamond electrode and by Wang et al. [56] on a porous graphite electrode. In addition under acidic conditions the active chlorine is mainly present as hypochlorous acid which is a stronger oxidant towards organic species than hypochlorite [57].

In the Na_2SO_4 containing system, pH and anode material have limited effects on the TOC removal percentage while the flow velocity plays a dominant role. The TOC removal percentage at 600 ml min^{-1} was found to be higher than at 60 ml min^{-1}. This result reveals that the electrochemical reaction rate is controlled primarily by mass transfer limitations.

In the NaCl containing system, the effects of pH on the TOC removal percentage are more pronounced. When PbO_2/Ti was used as the anode, the effect of pH and flow velocity followed the same trend, i.e. in either acidic or basic conditions, high flow velocity favored electrooxidation. Using the PbO_2/NT, a higher TOC removal percentage was obtained in acidic conditions when flow rate was 600 ml min^{-1}. While in basic conditions, the flow rate at 60 ml min^{-1} favors the TOC removal in comparison to the flow rate at 600 ml min^{-1}. One possible explanation might be the properties of microstructure of the NT arrays, which restricted the diffusion of the bulk electrolyte. Therefore, the pH of the solution inside NT would be blocked from the pH of the bulk solution. Along with the splitting of water near the anode surface, the pH of the solution inside NT decreased until it reached a steady value. It is known that lower pH favors chlorine oxidation, which will assist electrochemical degradation of TOC as is shown in Fig. 5b. These results are analogous to those obtained by Trasatti [58] who used RuO_2, Co_3O_4 and $NiCo_2O_4$ anodes.

4. Conclusions

TiO_2 NT arrays were fabricated using anodic oxidation of Ti sheets in fluoride containing electrolyte. A layer of PbO_2 was deposited on the TiO_2 NT arrays substrate by the procedure of PED technique. The characterization and catalytic property tests were carried out and the results revealed the following:

- The predominant phase of the PbO_2/NT anode is β-PbO_2.
- There is an optimum length of electrodeposition time for PbO_2/NT under the operating conditions used in this study.
- The microstructure of anode materials drastically impacts the results of chronoamperometric experiments in the presence of NaCl. The apparent current on the PbO_2/Ti first declined then increased with increasing NaCl concentration in alkaline solutions. However, the apparent current on the PbO_2/NT increased throughout the process of increasing the NaCl concentration.
- The effect of current density on the TOC removal percentage is different when the reactant is different. The TOC removal percentage of isopropanol is mainly affected by mass transfer control, whereas the effect of anode passivation caused by 4-CP played a more important role than the effect of mass transfer in the electrochemical incineration experiment. The passivation phenomenon was confirmed by cyclic voltammetry measurement.
- Degradation experiments that were carried out in a hydraulic circuit system showed that electrochemical oxidation occurred at a much faster rate than in the case of sulphate-based electrolytes. PbO_2/NT was more efficient than PbO_2/Ti in converting the isopropanol into carbonate, bicarbonate or CO_2.
- The nature of the surpporting electrolyte (Na_2SO_4, NaCl) influenced the electrochemical oxidation process. In the Na_2SO_4 containing system, on both of the electrodes, higher abatement of TOC was obtained under large flow velocity regardless of pH. When NaCl was used as the supporting electrolyte, high flow velocity favored electrooxidation in the case of PbO_2/Ti. While in the case of PbO_2/NT, high flow velocity in acidic conditions or low flow velocity in basic conditions favored the TOC removal.

Acknowledgements

The authors would like to give special thanks to Mr. Case van Genuchten at University of California, Berkeley, United States for his revision of the language and helpful discussions. This work is supported by the National Natural Science Foundation of China (No. 20577034).

References

[1] C.A. Silva, L.M. Madeira, R.A. Boaventura, C.A. Costa, Photo-oxidation of cork manufacturing wastewater, Chemosphere 55 (2004) 19–26.
[2] F.J. Beltran, J.F. Garcia-Araya, J. Frades, P. Alvarez, O. Gimeno, Effects of single and combined ozonation with hydrogen peroxide or UV radiation on the chemical degradation and biodegradability of debittering table olive industrial wastewaters, Water Res. 33 (1999) 723–732.
[3] A.G. Chakinala, P.R. Gogate, A.E. Burgess, D.H. Bremner, Industrial wastewater treatment using hydrodynamic cavitation and heterogeneous advanced Fenton processing, Chem. Eng. J. 152 (2009) 498–502.
[4] L. Ma, W.-x. Zhang, Enhanced biological treatment of industrial wastewater with bimetallic zero-valent iron, Environ. Sci. Technol. 42 (2008) 5384–5389.
[5] E.M. Sulman, V.G. Matveeva, V.Y. Doluda, A.I. Sidorov, N.V. Lakina, A.V. Bykov, M.G. Sulman, P.M. Valetsky, L.M. Kustov, O.P. Tkachenko, B.D. Stein, L.M. Bronstein, Efficient polymer-based nanocatalysts with enhanced catalytic performance in wet air oxidation of phenol, Appl. Catal. B: Environ. 94 (2009) 200–210.
[6] Y.-h. Cui, X.-y. Li, G. Chen, Electrochemical degradation of bisphenol A on different anodes, Water Res. 43 (2009) 1968–1976.
[7] M. Panizza, G. Cerisola, Electrocatalytic materials for the electrochemical oxidation of synthetic dyes, Appl. Catal. B: Environ. 75 (2007) 95–101.
[8] X. Yang, R. Zou, F. Huo, D. Cai, D. Xiao, Preparation and characterization of Ti/SnO_2–Sb_2O_3–Nb_2O_5/PbO_2 thin film as electrode material for the degradation of phenol, J. Hazard. Mater. 164 (2009) 367–373.
[9] X.-y. Li, Y.-h. Cui, Y.-j. Feng, Z.-m. Xie, J.-D. Gu, Reaction pathways and mechanisms of the electrochemical degradation of phenol on different electrodes, Water Res. 39 (2005) 1972–1981.
[10] x. Marti, C.A. nez-Huitle, A. De Battisti, S. Ferro, S. Reyna, L. Cerro, M. pez, nica, M.A. Quiro, Removal of the pesticide methamidophos from aqueous solutions by electrooxidation using Pb/PbO_2, Ti/SnO_2, and Si/BDD electrodes, Environ. Sci. Technol. 42 (2008) 6929–6935.
[11] A. Sakalis, D. Vanerkov, M. Holcapek, P. Jandera, A. Voulgaropoulos, Electrochemical treatment of a simple azodye and analysis of the degradation products using high performance liquid chromatography-diode array detection-tandem mass spectrometry, Chemosphere 67 (2007) 1940–1948.
[12] L. Szpyrkowicz, S.N. Kaul, R.N. Neti, S. Satyanarayan, Influence of anode material on electrochemical oxidation for the treatment of tannery wastewater, Water Res. 39 (2005) 1601–1613.
[13] C. Zhang, J. Wang, H. Zhou, D. Fu, Z. Gu, Anodic treatment of acrylic fiber manufacturing wastewater with boron-doped diamond electrode: a statistical approach, Chem. Eng. J. 161 (2010) 93–98.
[14] M.J.K. Bashir, M.H. Isa, S.R.M. Kutty, Z.B. Awang, H.A. Aziz, S. Mohajeri, I.H. Farooqi, Landfill leachate treatment by electrochemical oxidation, Waste Manage. (Oxford) 29 (2009) 2534–2541.
[15] L. Gomes, R.G. Freitas, G.R.P. Malpass, E.C. Pereira, A.J. Motheo, Pt film electrodes prepared by the Pechini method for electrochemical decolourisation of Reactive Orange 16, J. Appl. Electrochem. 39 (2009) 117–121.
[16] R. Tolba, M. Tian, J. Wen, Z.-H. Jiang, A. Chen, Electrochemical oxidation of lignin at IrO_2-based oxide electrodes, J. Electroanal. Chem. (2010), doi:10.1016/j.jelechem.2009.12.013.

[17] J. Gaudet, A.C. Tavares, S. Trasatti, D. Guay, Physicochemical characterization of mixed RuO_2–SnO_2 solid solutions, Chem. Mater. 17 (2005) 1570–1579.
[18] B. Adams, M. Tian, A. Chen, Design and electrochemical study of SnO_2-based mixed oxide electrodes, Electrochim. Acta 54 (2009) 1491–1498.
[19] F. Bonfatti, S. Ferro, F. Lavezzo, M. Malacarne, G. Lodi, A. De Battisti, Electrochemical incineration of glucose as a model organic substrate I. Role of the electrode material, J. Electrochem. Soc. 146 (1999) 2175–2179.
[20] L. Ciriaco, C. Anjo, J. Correia, M.J. Pacheco, A. Lopes, Electrochemical degradation of Ibuprofen on Ti/Pt/PbO_2 and Si/BDD electrodes, Electrochim. Acta 54 (2009) 1464–1472.
[21] I. Sires, E. Brillas, G. Cerisola, M. Panizza, Comparative depollution of mecoprop aqueous solutions by electrochemical incineration using BDD and PbO_2 as high oxidation power anodes, J. Electroanal. Chem. 613 (2008) 151–159.
[22] C. Borras, T. Laredo, J. Mostany, B.R. Scharifker, Study of the oxidation of solutions of p-chlorophenol and p-nitrophenol on Bi-doped PbO_2 electrodes by UV–vis and FTIR in situ spectroscopy, Electrochim. Acta 49 (2004) 641–648.
[23] N. Popovic, J.A. Cox, D.C. Johnson, A mathematical model for anodic oxygen-transfer reactions at Bi(V)-doped PbO_2-film electrodes, J. Electroanal. Chem. 456 (1998) 203–209.
[24] L.S. Andrade, R.C. Rocha-Filho, N. Bocchi, S.R. Biaggio, J. Iniesta, V. Garcia-Garcia, V. Montiel, Degradation of phenol using Co- and Co, F-doped PbO_2 anodes in electrochemical filter-press cells, J. Hazard. Mater. 153 (2008) 252–260.
[25] Y. Song, G. Wei, R. Xiong, Structure and properties of PbO_2–CeO_2 anodes on stainless steel, Electrochim. Acta 52 (2007) 7022–7027.
[26] S. Ai, M. Gao, W. Zhang, Q. Wang, Y. Xie, L. Jin, Preparation of Ce–PbO_2 modified electrode and its application in detection of anilines, Talanta 62 (2004) 445–450.
[27] L.S. Andrade, L.A.M. Ruotolo, R.C. Rocha-Filho, N. Bocchi, S.R. Biaggio, J. Iniesta, V. Garcia-Garcia, V. Montiel, On the performance of Fe and Fe, F doped Ti–Pt/PbO_2 electrodes in the electrooxidation of the Blue Reactive 19 dye in simulated textile wastewater, Chemosphere 66 (2007) 2035–2043.
[28] S.-P. Tong, C.-A. Ma, H. Feng, A novel PbO_2 electrode preparation and its application in organic degradation, Electrochim. Acta 53 (2008) 3002–3006.
[29] J. Cao, H. Zhao, F. Cao, J. Zhang, C. Cao, Electrocatalytic degradation of 4-chlorophenol on F-doped PbO_2 anodes, Electrochim. Acta 54 (2009) 2595–2602.
[30] M. Zhou, J. He, Degradation of cationic red X-GRL by electrochemical oxidation on modified PbO_2 electrode, J. Hazard. Mater. 153 (2008) 357–363.
[31] M.F. Brugnera, K. Rajeshwar, J.C. Cardoso, M.V.B. Zanoni, Bisphenol, A removal from wastewater using self-organized TiO_2 nanotubular array electrodes, Chemosphere 78 (2009) 569–575.
[32] G.H. Zhao, X. Cui, M.C. Liu, P.Q. Li, Y.G. Zhang, T.C. Cao, H.X. Li, Y.Z. Lei, L. Liu, D.M. Li, Electrochemical degradation of refractory pollutant using a novel microstructured TiO_2 nanotubes/Sb-doped SnO_2 electrode, Environ. Sci. Technol. 43 (2009) 1480–1486.
[33] D.M. Willberg, P.S. Lang, R.H. Hochemer, A. Kratel, M.R. Hoffmann, Degradation of 4-chlorophenol, 3,4-dichloroaniline, and 2,4,6-trinitrotoluene in an electrohydraulic discharge reactor, Environ. Sci. Technol. 30 (1996) 2526–2534.
[34] E. Brillas, M.A. Banos, M. Skoumal, P.L. Cabot, J.A. Garrido, R.M. Rodriguez, Degradation of the herbicide 2,4-DP by anodic oxidation, electro-Fenton and photoelectro-Fenton using platinum and boron-doped diamond anodes, Chemosphere 68 (2007) 199–209.
[35] G.G. Zhang, H.T. Huang, Y.S. Liu, L.M. Zhou, Fabrication of crack-free anodic nanoporous titania and its enhanced photoelectrochemical response, Appl. Catal. B: Environ. 90 (2009) 262–267.
[36] J.M. Macak, B.G. Gong, M. Hueppe, P. Schmuki, Filling of TiO_2 nanotubes by self-doping and electrodeposition, Adv. Mater. 19 (2007) 3027–3031.
[37] Y. Zhang, Y. Yang, P. Xiao, X. Zhang, L. Lu, L. Li, Preparation of Ni nanoparticle-TiO_2 nanotube composite by pulse electrodeposition, Mater. Lett. 63 (2009) 2429–2431.
[38] J. Cao, H. Zhao, F. Cao, J. Zhang, The influence of F^- doping on the activity of PbO_2 film electrodes in oxygen evolution reaction, Electrochim. Acta 52 (2007) 7870–7876.
[39] K.T. Kawagoe, D.C. Johnson, Electrocatalysis of anodic oxygen-transfer reactions, J. Electrochem. Soc. 141 (1994) 3404–3409.
[40] M. Zhou, Q. Dai, L. Lei, M.A. Chun'an, D. Wang, Long life modified lead dioxide anode for organic wastewater treatment: electrochemical characteristics and degradation mechanism, Environ. Sci. Technol. 39 (2005) 363–370.
[41] X.P. Zhu, M.P. Tong, S.Y. Shi, H.Z. Zhao, J.R. Ni, Essential explanation of the strong mineralization performance of boron-doped diamond electrodes, Environ. Sci. Technol. 42 (2008) 4914–4920.
[42] Y. Liu, H. Liu, J. Ma, X. Wang, Comparison of degradation mechanism of electrochemical oxidation of di- and tri-nitrophenols on Bi-doped lead dioxide electrode: effect of the molecular structure, Appl. Catal. B: Environ. 91 (2009) 284–299.
[43] O. Scialdone, S. Randazzo, A. Galia, G. Silvestri, Electrochemical oxidation of organics in water: role of operative parameters in the absence and in the presence of NaCl, Water Res. 43 (2009) 2260–2272.
[44] Z. Zhang, G. Zhao, X. Luo, Y. Xu, Introduction of Titanium Electrode, Metallurgical Industry Press, Beijing, 2008.
[45] C.N. Reshef Tenne, R. Rao, Inorganic nanotubes, Philos. Trans. R. Soc. A 362 (2004) 2099.
[46] G.K. Mor, O.K. Varghese, M. Paulose, K. Shankar, C.A. Grimes, A review on highly ordered, vertically oriented TiO_2 nanotube arrays: fabrication, material properties, and solar energy applications, Sol. Energy Mater. Sol. Cells 90 (2006) 2011–2075.
[47] R.A. Torres, W. Torres, P. Peringer, C. Pulgarin, Electrochemical degradation of p-substituted phenols of industrial interest on Pt electrodes. Attempt of a structure–reactivity relationship assessment, Chemosphere 50 (2003) 97–104.
[48] Y.H. Wang, K.Y. Chan, X.Y. Li, S.K. So, Electrochemical degradation of 4-chlorophenol at nickel-antimony doped tin oxide electrode, Chemosphere 65 (2006) 1087–1093.
[49] M. Hamza, R. Abdelhedi, E. Brillas, I. Sires, Comparative electrochemical degradation of the triphenylmethane dye Methyl Violet with boron-doped diamond and Pt anodes, J. Electroanal. Chem. 627 (2009) 41–50.
[50] M.O. Azzam, M. Al-Tarazi, Y. Tahboub, Anodic destruction of 4-chlorophenol solution, J. Hazard. Mater. 75 (2000) 99–113.
[51] N.B. Tahar, A. Savall, Electrochemical removal of phenol in alkaline solution. Contribution of the anodic polymerization on different electrode materials, Electrochim. Acta 54 (2009) 4809–4816.
[52] R. Sripriya, M. Chandrasekaran, K. Subramanian, K. Asokan, M. Noel, Electrochemical destruction of p-chlorophenol and p-nitrophenol – influence of surfactants and anode materials, Chemosphere 69 (2007) 254–261.
[53] H. Park, C.D. Vecitis, M.R. Hoffmann, Solar-powered electrochemical oxidation of organic compounds coupled with the cathodic production of molecular hydrogen, J. Phys. Chem. A 112 (2008) 7616–7626.
[54] K.V. Radha, V. Sridevi, K. Kalaivani, Electrochemical oxidation for the treatment of textile industry wastewater, Bioresour. Technol. 100 (2009) 987–990.
[55] C. Flox, J.A. Garrido, R.M. Rodriuez, F. Centellas, P.-L. Cabot, C. Arias, E. Brillas, Degradation of 4,6-dinitro-o-cresol from water by anodic oxidation with a boron-doped diamond electrode, Electrochim. Acta 50 (2005) 3685–3692.
[56] B. Wang, X. Chang, H. Ma, Electrochemical oxidation of refractory organics in the coking wastewater and chemical oxygen demand (COD) removal under extremely mild conditions, Ind. Eng. Chem. Res. 47 (2008) 8478–8483.
[57] M. Deborde, U. von Gunten, Reactions of chlorine with inorganic and organic compounds during water treatment – kinetics and mechanisms: a critical review, Water Res. 42 (2008) 13–51.
[58] S. Trasatti, Progress in the understanding of the mechanism of chlorine evolution at oxide electrodes, Electrochim. Acta 32 (1987) 369–382.